The Photogravitational Circular Restricted Four-body Problem with Variable Masses

Abdullah A. Ansari

Department of Mathematics , College of Science, Majmaah University, Al-Zulfi, Kingdom of Saudi Arabia,

a.ansari@mu.edu.sa

Abstract

In this paper, we examine the stability of the equilibrium points in the photogravitational circular restricted four-body problem by considering all the masses are varying with time, one of the three masses are taken as source of radiation pressure and all the masses are placed at the vertices of an equilateral triangle. We derive the equations of motion under the effect of solar radiation pressure by using the Meshcherskii transformations. We have plotted the equilibrium points, time series, surfaces of motion of infinitesimal body, Poincare surface of sections and Newton-Raphson basin of attraction. Here five equilibrium points are found but it is ten in the classical case. From the time series, it is observed that the orbit will not be periodic. The surfaces of motion of the infinitesimal body are studied in the space. The Poincare surface of section is in the discrete type of pattern. The convergence of the equilibrium points is studied by the Newton-Raphson basin of attraction. Finally, we have examined the stability of the equilibrium points and found that all the equilibrium points are unstable.

Keywords: Radiation Pressure; variable masses; equilateral triangle; Poincare surface of sections; Newton-Raphson basin of attraction.

1. Introduction

The restricted problem is studied by many scientists and mathematicians in the two-body, three-body, four-body and N-body models. Chernikov [8] investigated the stability of equilibrium points by Lyapunov's methods in the restricted three body problem (Sun-Planet-Particle) with the effects of solar radiation pressure. Perezhogin [17] studied the stability of the sixth and seventh libration points in the photogravitational circular restricted three body problem. Bhatnagar et al. [7] studied about the lagrangian points in the photogravitational restricted three body problem. They examined the stability of the equilibrium points and observed that the equilibrium points are stable in the linear sense and unstable around the triangular points. Mignard [14] studied the restricted three-body problem with the inclusion of solar radiation pressure. And observed that triangular equilibrium points are no longer exist. Simmons [20] investigated the restricted 3-body problem with radiation pressure and observed that nine equilibrium points exists, five in the plane of motion and four in the out of plane. Sharma [19] investigated the variation of the solar radiation pressure and oblateness factor on the stationary solutions of the planar restricted three-body problem when the more massive primary is a source of radiation and smaller primary is an oblate spheroid with its equatorial plane coincident with the plane of motion. AbdulRaheem et al. [4] investigated the stability of equilibrium points under the influence of the Coriolis and centrifugal forces together with the effects of oblateness and radiation pressure of the primaries. It is observed that the collinear points are unstable and the triangular points are conditionally stable depending on the radiation factor and oblateness. It is also observed that the Coriolis force has a stabilizing tendency, while the centrifugal force, radiation and oblateness of the primaries have destabilizing effects. Kalvouridis, et al. [10] investigated the dynamical properties and the parametric evolution of periodic orbits in the restricted four body problem with radiation pressure. They illustrated the zero-velocity curves and surfaces and also they examined the stability of the equilibrium points. Abouelmagd [2] investigated the stability and periodic orbits in the restricted three body problem under the effects of oblateness and radiation pressure. He observed that the collinear points are unstable while triangular points are conditionally stable depending on the radiation pressure and oblateness. And also the elements of periodic orbits around equilibrium points are affected by oblateness. Singh, et al. [25] studied numerically the restricted four-body problem by considering all the primaries as source of radiation pressure, placed at the vertices of an equilateral triangle. They observed that the equilibrium points are unstable. Pushparaj, et al. [18] studied the interior resonance periodic orbits around the Sun in the photogravitational restricted three body problem by the method of Poincare surface of section. They observed that the period of time decrease with the increase of radiation pressure.

Many researchers have explored about the variable masses and the Newton-Raphson basins of attraction as Meshcherskii [13], Lichtenegger[12] Singh [21, 22, 23, 24], Douskos [9], Zhang [26], Kumari [11], Assis [5], Abouelmagd [3], Mittal [15], Zotos [27, 28, 29, 30].

We have studied the circular restricted four-body problem in which the masses of the primaries as well as the mass of the infinitesimal body vary with time and one of the primaries is taken as source of radiation pressure. We have discussed our problem in various sections. In the first section, we have reviewed the literature. In the second section, we have derived the equations of motion of the infinitesimal variable mass under the effects of the radiation pressure. In the third section, we have illustrated the numerical analysis (equilibrium points, time series, surface of motion of the infinitesimal body, Poincare surface of section and Newton-Raphson basin of attraction). In the fourth section, we have examined the stability of the equilibrium points. Finally, in the fifth section, we have concluded the problem. Our problem has great applications in the Astronomy and Astrophysics.

2. Equations of motion

Let m_1, m_2 and m_3 be the masses of the three primaries, placed at the vertices of an equilateral triangle of side ℓ. The fourth infinitesimal body having mass m, moving under the influence of the primaries but not influencing them. The one of the primaries as m_2 is considered as source of radiation pressure with factor q and all the masses are varying with time. The primaries are revolving in the circular orbits around their center of mass which is considered as origin. The primary m_1 is placed at x-axis, the line passing through the origin and perpendicular to the x-axis, is taken as y-axis and the line passing through the origin and perpendicular to the plane of motion of the primaries is taken as z-axis (Fig. 1). Initially, we supposed that the synodic plane coincides with the inertial plane and revolving with mean motion ω about z-axis. Using the procedure of Abdullah [1], we can write the equations of motion of the variable infinitesimal body in the restricted four body problem as

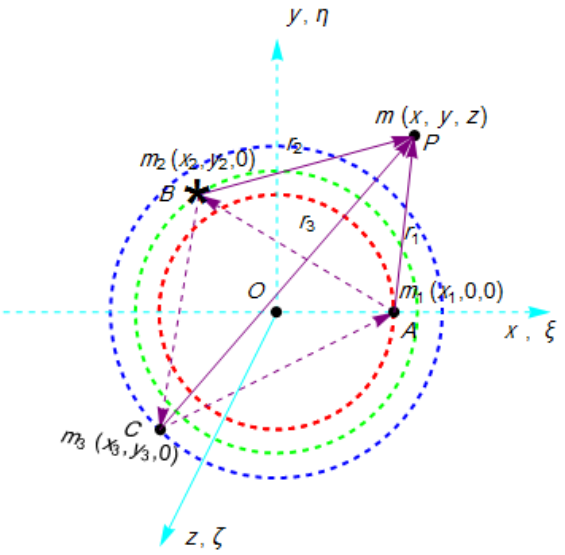

Fig. 1: Configuration of the circular restricted four-body problem with solar radiation pressure at B.

$$\frac{\dot{m}}{m}(\dot{x}-\omega\, y)+(\ddot{x}-\dot{\omega}\, y\, -2\omega\, \dot{y}-\omega^2 x)=$$
$$-\frac{m_1G(x-x_1)}{r_1^3}-\frac{m_2G(x-x_2)q}{r_2^3}-\frac{m_3G(x-x_3)}{r_3^3},$$

$$\frac{\dot{m}}{m}(\dot{y}+\omega x)+(\ddot{y}+\dot{\omega}x\, +2\omega\, \dot{x}\, -\omega^2 y)=$$
$$-\frac{m_1G(y-y_1)}{r_1^3}-\frac{m_2G(y-y_2)q}{r_2^3}-\frac{m_3G(y-y_3)}{r_3^3},$$
$$\frac{\dot{m}}{m}\dot{z}+\ddot{z}=-\frac{m_1Gz}{r_1^3}-\frac{m_2Gzq}{r_2^3}-\frac{m_3Gz}{r_3^3},$$

where,

$r_i^2=(x-x_i)^2+(y-y_i)^2+z^2,(i=1,2,3)$, are the distances from the primaries to the infinitesimal body, G is the gravitational constant.

Let $\mu_i(t)=m_iG,(i=1,2,3).$

Using Meshcherskii transformation [13],

$$x=\xi R(t),\ y=\eta R(t),\ z=\zeta R(t),$$
$$\frac{dt}{d\tau}=R^2(t),\ r_i=\rho_i R(t),$$
$$\omega(t)=\frac{\omega_0}{R^2(t)},\ x_i=\xi_i R(t),\ y_i=\eta_i R(t),$$

$$\mu(\mathrm{t}) = \frac{\mu_0}{R(\mathrm{t})}, \mu_i(\mathrm{t}) = \frac{\mu_{i0}}{R(\mathrm{t})},$$
$$\mathrm{m} = \frac{m_0}{R(\mathrm{t})}, R(\mathrm{t}) = \sqrt{a\,t^2 + 2b\,t + c},$$
$$ac - b^2 = 1 - k, \quad (i = 1,2,3),$$

where k $a, b, c, \mu_0, \mu_{10}, \mu_{20}, \mu_{30}, \mathrm{m}_0$ are constants.

Considering unit of mass, distance and time at initial time t_0 such that

$$\mu_0 = 1, \ell = 1, \omega_0 = 1, G = 1, \mathrm{a}\,t_0 + b = \alpha_1(\text{constant})$$

Introducing the mass parameter as

$$\mu_{10} = \mu, \ \mu_{20} = (1 - \mu - \alpha_2\mu), \ \mu_{30} = \alpha_2\mu, \ \ \alpha_2 << 1,$$

Finally, the equations of motion become

$$\xi'' - 2\eta' - \alpha_1\xi' = \Omega_\xi,$$
$$\eta'' + 2\xi' - \alpha_1\eta' = \Omega_\eta,$$
$$\zeta'' - \alpha_1\zeta' = \Omega_\zeta. \qquad (1)$$

where,

$$\Omega = \frac{1}{2}(\alpha_1^2 + k)(\xi^2 + \eta^2 + \zeta^2) - \frac{1}{2}\zeta^2$$
$$- \alpha_1\,\xi\,\eta + \frac{\mu}{} + \frac{(1 - \mu - \alpha_2\mu)\,\mathrm{q}}{} + \frac{\alpha_2\mu}{\rho_3},$$
$$\rho_i^2 = (\xi - \xi_i)^2 + (\eta - \eta_i)^2 + \zeta^2,$$

$$(\xi_1, \eta_1) = (\tfrac{1}{\sqrt{3}}, 0), (\xi_2, \eta_2) = (-\tfrac{1}{2\sqrt{3}}, \tfrac{1}{2}),$$
$$(\xi_3, \eta_3) = (-\tfrac{1}{2\sqrt{3}}, -\tfrac{1}{2}).$$

Prime (‘) is the differentiation w.r.t. τ .

3. Numerical Analysis

3.1 Equilibrium points

The equilibrium points can found by taking $\xi'' = \xi' = \eta'' = \eta' = \zeta'' = \zeta' = 0$ in equation (1), i.e.

$$(\alpha_1^2 + k)\xi - \alpha_1\eta - \frac{\mu(\xi - \xi_1)}{\rho_1^3}$$
$$- \frac{(1 - \mu - \alpha_2\mu)(\xi - \xi_2)q}{\rho_2^3} - \frac{\alpha_2\mu(\xi - \xi_3)}{\rho_3^3} = 0, \quad (2)$$

$$(\alpha_1^2 + k)\eta - \alpha_1\xi - \frac{\mu\eta}{\rho_1^3}$$
$$- \frac{(1 - \mu - \alpha_2\mu)(\eta - \eta_2)q}{\rho_2^3} - \frac{\alpha_2\mu(\eta - \eta_3)}{\rho_3^3} = 0, \quad (3)$$

$$(\alpha_1^2 + k - 1)\zeta - \frac{\mu\zeta}{\rho_1^3} - \frac{(1 - \mu - \alpha_2\mu)\zeta q}{\rho_2^3}$$
$$- \frac{\alpha_2\mu\zeta}{\rho_3^3} = 0. \quad (4)$$

We have shown the equilibrium points graphically in (ξ, η) plane (Fig. 2), (ξ, ζ) plane (Fig. 3) and (η, ζ) plane (Fig. 4). In the (ξ, η) plane, we found five equilibrium points. The green dots denote the locations of the equilibrium points and the purple dots denote the locations of the primaries. But Baltagiannis [6] have gotten ten equilibrium points with unequal masses in the classical case. In the (ξ, ζ) plane, we found five equilibrium points. The green dots denote the locations of the equilibrium points. In the (η, ζ) plane, we found three equilibrium points. The black dots denote the locations of the equilibrium points.

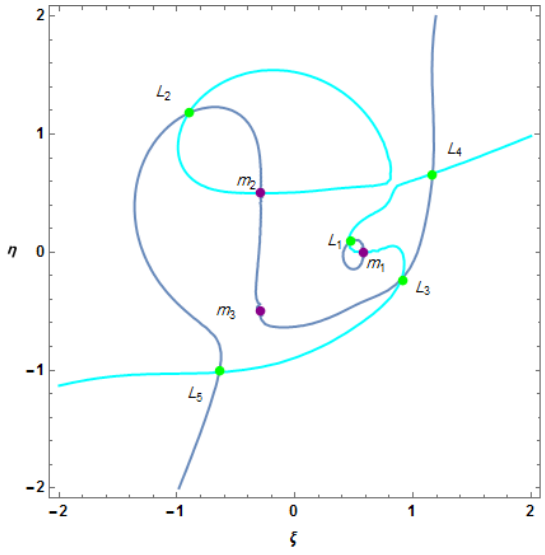

Fig. 2: Locations of equilibrium points at

$\alpha_1 = 0.2, k = 0.4, \alpha_2 = 0.01, \mu = 0.019, q = 0.8.$

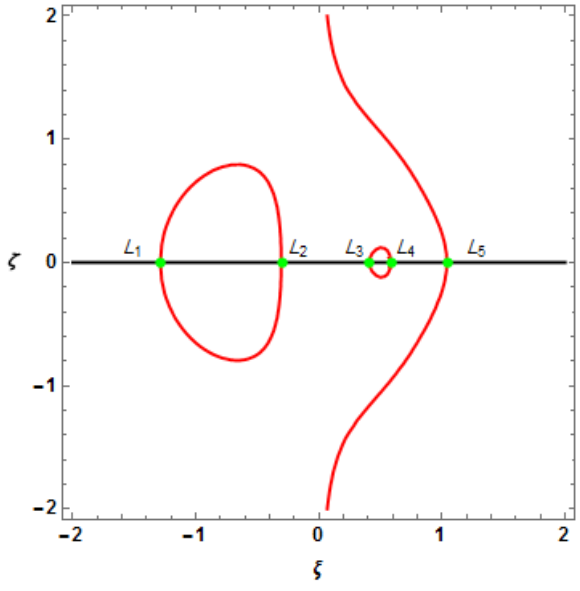

Fig. 3. Locations of equilibrium points at

$\alpha_1 = 0.2, k = 0.4, \alpha_2 = 0.01, \mu = 0.019, q = 0.8.$

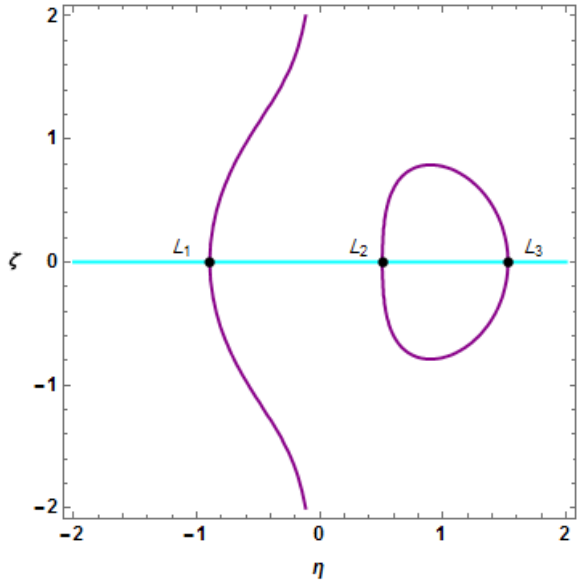

Fig. 4. Locations of equilibrium points at

$\alpha_1 = 0.2, k = 0.4, \alpha_2 = 0.01, \mu = 0.019, q = 0.8.$

3.2 Time series

We have plotted the time series in between (τ, ξ) (Fig. 5.) and (τ, η) (Fig. 6). These time series show that the orbits will not be periodic.

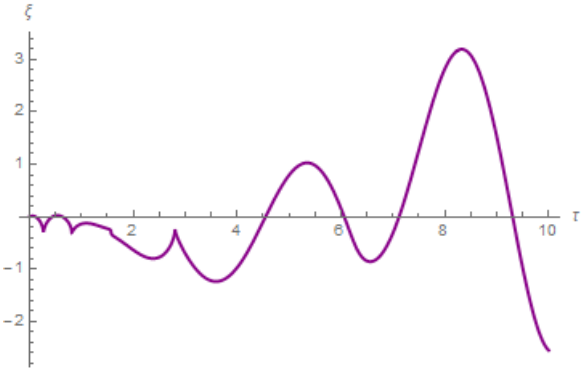

Fig. 5. Time series in between (τ, ξ) at

$\alpha_1 = 0.2, k = 0.4, \alpha_2 = 0.01, \mu = 0.019, q = 0.8.$

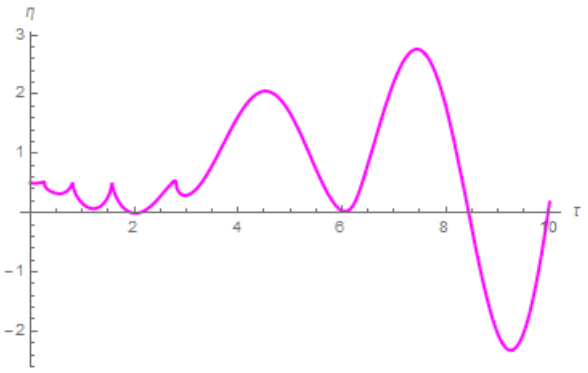

Fig. 6. Time series in between (τ,η) at

$\alpha_1 = 0.2, k = 0.4, \alpha_2 = 0.01, \mu = 0.019, q = 0.8.$

3.3 Surfaces

i.Surfaces of the motion of the infinitesimal body

In this section, we have drawn the surface of motion of the infinitesimal body by considering the equations (2 and 3) (Fig. 7), the equations (2 and 4) (Fig. 8), the equations (3 and 4) (Fig. 9).

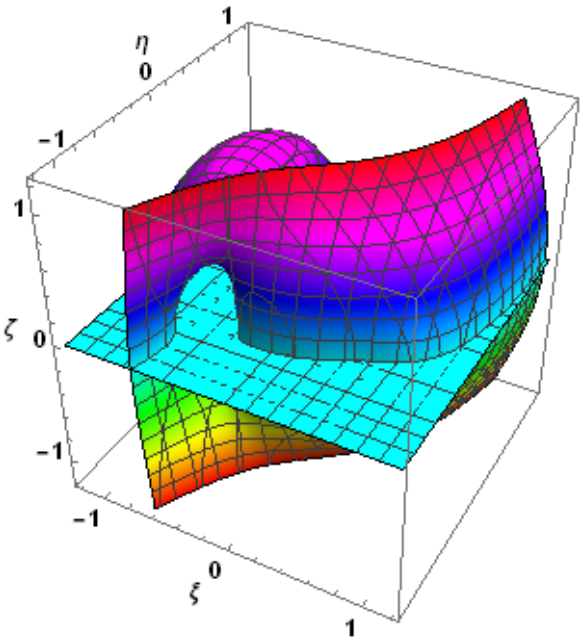

Fig. 8. The surface of motion of the infinitesimal body in $(\xi,\eta=0,\zeta)$ -plane

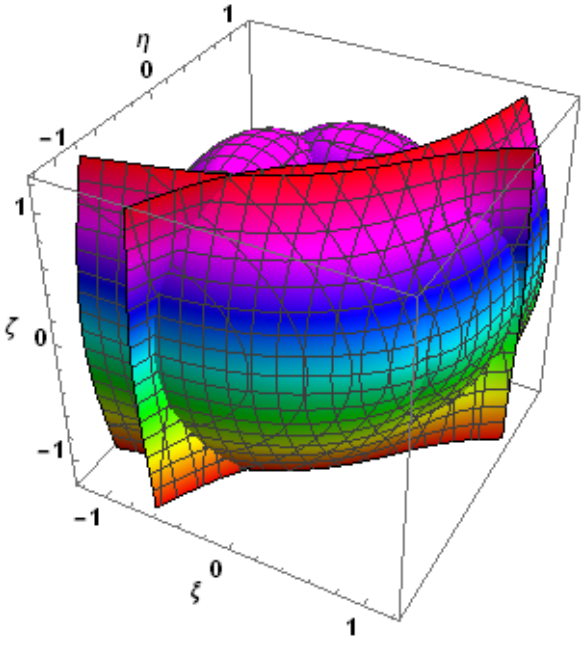

Fig. 7. The surface of motion of the infinitesimal body in $(\xi,\eta,\zeta=0)$ -plane

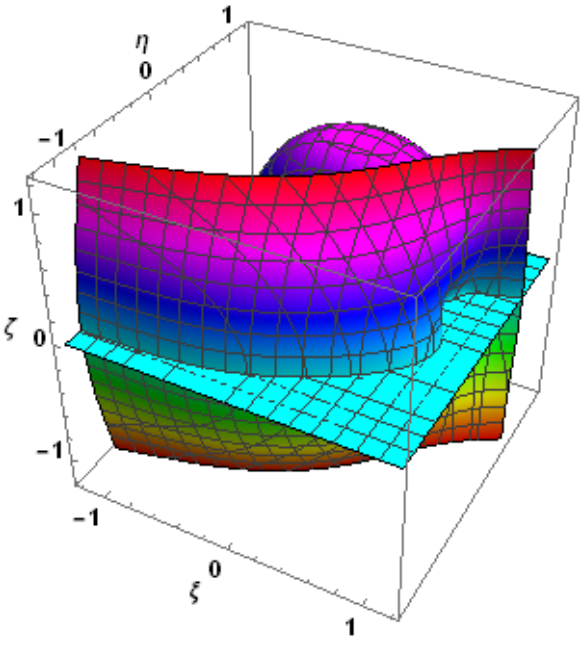

Fig. 9. The surface of motion of the infinitesimal body in $(\xi=0,\eta,\zeta)$ -plane

ii. Poincare surface of section

We have drawn the Poincare surface of section and got a discrete type of graph (Fig. 10).

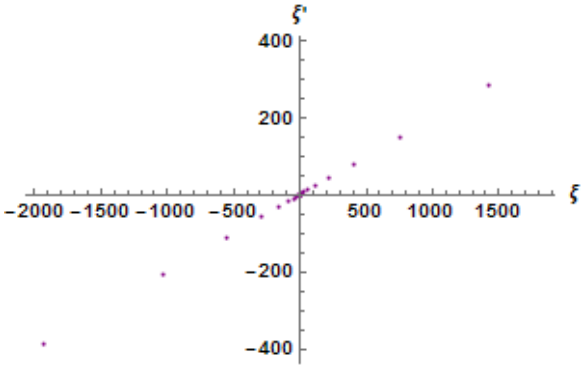

Fig. 10: Poincare surface of section

3.4 Newton-Raphson basin of attraction

We have drawn the basins of attraction by using the simple and accurate Newton-Raphson iterative method for solving systems of equation. This method is also applicable for systems of multivariate functions. The iterative algorithm of our problem is given by the system

$$\xi_n = \xi_{n-1} - \left(\frac{\Omega_\xi \Omega_{\eta\eta} - \Omega_\eta \Omega_{\xi\eta}}{\Omega_{\xi\xi}\Omega_{\eta\eta} - \Omega_{\xi\eta}\Omega_{\eta\xi}} \right)_{(\xi_{n-1},\eta_{n-1})},$$

$$\eta_n = \eta_{n-1} - \left(\frac{\Omega_\eta \Omega_{\xi\xi} - \Omega_\xi \Omega_{\eta\xi}}{\Omega_{\xi\xi}\Omega_{\eta\eta} - \Omega_{\xi\eta}\Omega_{\eta\xi}} \right)_{(\xi_{n-1},\eta_{n-1})}. \quad (5)$$

Where ξ_{n-1}, η_{n-1} are the values of the ξ and η coordinates of the $(n-1)_{th}$ step of the Newton-Raphson iterative process. The initial point (ξ, η) is a member of the basin of attraction of the root if this point converges rapidly to one of the equilibrium points. This process stops when the successive approximation converges to an attractor, with some predefined accuracy. For the classification of the equilibrium points on the (ξ, η) plane, we will use color code. In this way a complete view of the basin structures created by the attractors (Fig. 11). Also we have shown the zoomed part of the basins of attractions near the primaries (Fig. 12). We used Mathematica software for finding basin of attraction.

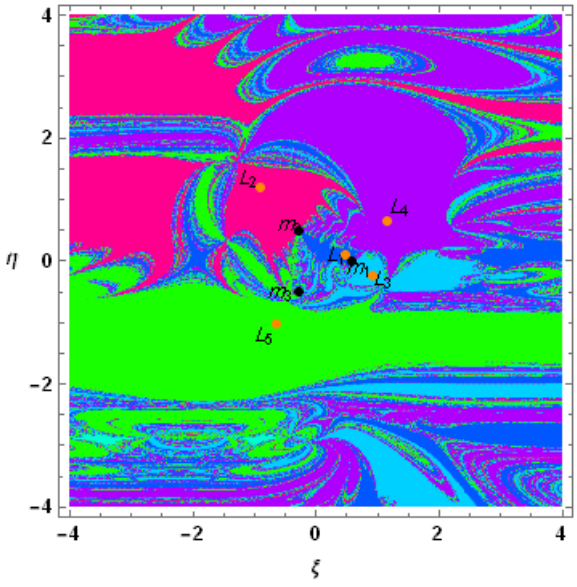

Fig. 11: Newton-Raphson basin of attraction under the effects of solar radiation pressure where orange dots indicate the locations of the equilibrium points and black dots indicate the locations of the primaries.

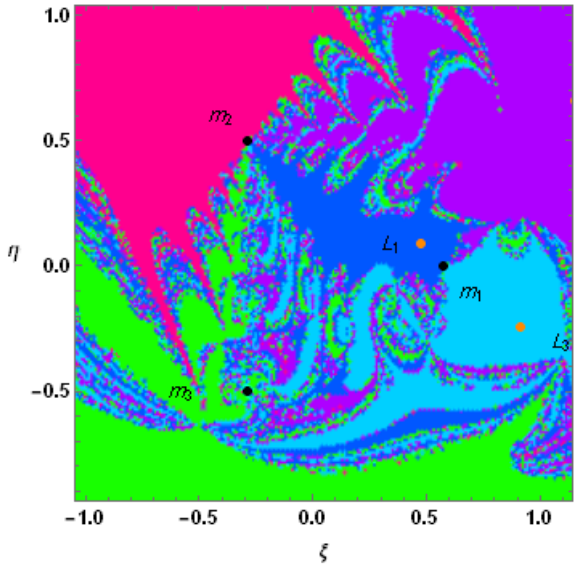

Fig. 12: The zoomed part of Fig. 11 near the primaries.

4. Stability

Using the procedure given by Mccuskey [16], we can examine the stability of the equilibrium points in the photogravitational circular restricted four-body problem. Let us suppose

$\xi = \xi_0 + \alpha, \eta = \eta_0 + \beta, \zeta = \zeta_0 + \gamma,$ putting these values in equation (1), we get

$$\alpha'' - 2\beta' - \alpha_1\alpha' = \alpha\,\Omega^0_{\xi\xi} + \beta\,\Omega^0_{\xi\eta} + \gamma\,\Omega^0_{\xi\zeta},$$

$$\beta'' + 2\alpha' - \alpha_1\beta' = \alpha\,\Omega^0_{\eta\xi} + \beta\,\Omega^0_{\eta\eta} + \gamma\,\Omega^0_{\eta\zeta},$$

$$\gamma'' - \alpha_1\gamma' = \alpha\,\Omega^0_{\zeta\xi} + \beta\,\Omega^0_{\zeta\eta} + \gamma\,\Omega^0_{\zeta\zeta}, \qquad (6)$$

Where α, β and γ are the small displacements of the infinitesimal body from the equilibrium points. Suffix zero denotes the value at the equilibrium point.

To solve equation (6), let

$$\alpha = Ae^{\lambda\tau}, \beta = Be^{\lambda\tau}, \gamma = Ce^{\lambda\tau},$$

where A, B and C are parameters.

After substituting these values in equation (6), we get

$$A(\lambda^2 - \alpha_1\lambda - \Omega^0_{\xi\xi}) - \mathrm{B}(2\lambda + \Omega^0_{\xi\eta}) - \mathrm{C}\,\Omega^0_{\xi\zeta} = 0,$$

$$\mathrm{A}(2\lambda - \Omega^0_{\eta\xi}) + B(\lambda^2 - \alpha_1\lambda - \Omega^0_{\eta\eta}) - \mathrm{C}\,\Omega^0_{\eta\zeta} = 0,$$

$$-A\,\Omega^0_{\zeta\xi} - \mathrm{B}\,\Omega^0_{\zeta\eta} + C(\lambda^2 - \alpha_1\lambda - \Omega^0_{\zeta\zeta}) = 0, \qquad (7)$$

The equation (7) will have a non-trivial solution for A, B and C, if

$$\begin{vmatrix} \lambda^2 - \alpha_1\lambda - \Omega^0_{\xi\xi} & -(2\lambda + \Omega^0_{\xi\eta}) & -\Omega^0_{\xi\zeta} \\ 2\lambda + \Omega^0_{\eta\xi} & \lambda^2 - \alpha_1\lambda - \Omega^0_{\eta\eta} & -\Omega^0_{\eta\zeta} \\ -\Omega^0_{\zeta\xi} & -\Omega^0_{\zeta\eta} & \lambda^2 - \alpha_1\lambda - \Omega^0_{\zeta\zeta} \end{vmatrix} = 0,$$

$$\begin{aligned} &\lambda^6 - 3\alpha_1\lambda^5 + \lambda^4(4 + 3\alpha_1^2 - \Omega^0_{\xi\xi} - \Omega^0_{\eta\eta} - \Omega^0_{\zeta\zeta}) \\ &+\lambda^3(-4\alpha_1 - \alpha_1^3 + 2\alpha_1\Omega^0_{\xi\xi} + 2\alpha_1\Omega^0_{\eta\eta} + 2\alpha_1\Omega^0_{\zeta\zeta} \\ &+4\Omega^0_{\xi\eta}) + \lambda^2((\Omega^0_{\xi\eta})^2 - (\Omega^0_{\xi\zeta})^2 + \Omega^0_{\xi\xi}\,\Omega^0_{\eta\eta} \\ &-(\Omega^0_{\eta\zeta})^2 - 4\Omega^0_{\zeta\zeta} + \Omega^0_{\xi\xi}\,\Omega^0_{\zeta\zeta} + \Omega^0_{\zeta\zeta}\Omega^0_{\eta\eta} \\ &+4\alpha_1\,\Omega^0_{\xi\eta} - \alpha_1^2(\Omega^0_{\xi\xi} + \Omega^0_{\eta\eta} + \Omega^0_{\zeta\zeta})) \\ &+\lambda(-4\Omega^0_{\xi\eta}\Omega^0_{\zeta\zeta} - \alpha_1(\Omega^0_{\xi\eta})^2 + \alpha_1(\Omega^0_{\xi\zeta})^2 \\ &-\alpha_1\,\Omega^0_{\xi\xi}\,\Omega^0_{\eta\eta} + \alpha_1(\Omega^0_{\eta\zeta})^2 - \alpha_1\Omega^0_{\xi\xi}\Omega^0_{\zeta\zeta} \\ &-\alpha_1\,\Omega^0_{\eta\eta}\,\Omega^0_{\zeta\zeta}) + ((\Omega^0_{\xi\zeta})^2\Omega^0_{\eta\eta} + \Omega^0_{\xi\xi}\,(\Omega^0_{\eta\zeta})^2 \\ &-(\Omega^0_{\xi\eta})^2\Omega^0_{\zeta\zeta} - \Omega^0_{\xi\xi}\,\Omega^0_{\eta\eta}\,\Omega^0_{\zeta\zeta}) = 0, \end{aligned} \qquad (8)$$

Table 1: Eigen Values

Coordinate of Equilibrium Points (ξ, η)	Eigen Values ($\lambda\lambda$)
L_1 $(0.34846,\ 0.09071)$	$\{-1.3645491647931514 - 2.1750266263845335i\}$, $\{-1.3645491647931514 + 2.1750266263845335i\}$, $\{0.1 - 1.9052998624502675i\}$, $\{0.1 + 1.9052998624502675i\}$, $\{0.915627074598914\}$, $\{2.2134712549873887\}\}$
L_2 $(-1.07658, 1.3532)$	$\{-0.4049887442604912 - 1.7442855728866289i\}$, $\{-0.4049887442604912 + 1.7442855728866289i\}$, $\{0.1 - 1.0261111757589274i\}$, $\{0.1 + 1.0261111757589274i\}$, $\{0.6049887442604907 - 0.2541475139791303i\}$, $\{0.6049887442604907 + 0.2541475139791303i$
L_3 $(1.07658, -0.30168)$ $(1.07658, -0.30168)$	$-0.17593511143553683 - 1.6967217827520438i\}$, $\{-0.17593511143553683 + 1.6967217827520438i\}$, $\{0.1 - 0.9185358306204258i\}$, $\{0.1 + 0.9185358306204258i\}$, $\{0.3759351114355368 - 0.28232515163735344i\}$, $\{0.3759351114355368 + 0.28232515163735344i\}$
L_4 $(1.36342, 0.873978)$	$\{0.012372274711160473 - 0.2854727328040165i\}$, $\{0.012372274711160473 + 0.2854727328040165i\}$, $\{0.1 - 0.8503875379646464i\}$, $\{0.1 + 0.8503875379646464i\}$, $\{0.18762772528883953 - 1.6913614606518697i\}$, $\{0.18762772528883953 + 1.6913614606518697i\}$
L_5 $(-0.8368, -1.1946)$	$\{0.009779043058938596 - 0.2850394466860824i\}$, $\{0.009779043058938596 + 0.2850394466860824i\}$, $\{0.1 - 0.831952106427792i\}$, $\{0.1 + 0.831952106427792i\}$, $\{0.19022095694106142 - 1.700849155153382i\}$, $\{0.19022095694106142 + 1.700849155153382i$

We solved the equation (8) for all the values of the equilibrium points and for each equilibrium point, we found six eigenvalues in which at least one is either positive real value or positive real part of the eigenvalues (Table 1). Therefore, all the equilibrium points are unstable.

5. Conclusions

In this paper, we explore the locations and stability of the circular restricted four-body problem by supposing all the masses are varying with time and one of the masses is source of radiation pressure. The three primaries are placed at the vertices of an equilateral triangle and revolving around their center of mass which is taken as origin. We derive the equations of

motion which are different from the classical case by the factors α_1 and k . We have plotted the graphs for the locations of the equilibrium points in three planes, the time series, the surfaces and the Newton-Raphson basin of attraction. In the (ξ, η) plane, we found five equilibrium points (Fig. 2) which are ten in the classical case, where the green dots denote the locations of the equilibrium points and the purple dots denote the locations of the primaries. In the (ξ, ζ) plane, we found five equilibrium points (Fig. 3) where the green dots denote the locations of the equilibrium points. In the (η, ζ) plane, we found three equilibrium points (Fig. 4) where the black dots denote the locations of the equilibrium points. From the time series, we observed that the orbits are not periodic (Fig. 5 & 6). We have drawn the surfaces of the motion of the infinitesimal body in three spaces (Figs. 7, 8, 9) and the Poincare surface of section where we got discrete type graph (Fig. 10). We also have drawn the Newton-Raphson basin of attraction (Fig. 11), where we have shown the convergence of the equilibrium points and the locations of equilibrium points are indicated by orange dots and the locations of the primaries are indicated by black dots. The Fig. 12 is the zoomed part of the Fig. 11 near the primaries. Zotos [27, 28, 29, 30] are illustrated basins of attraction in the classical case and they found scorpion type graph which is different from my case. Finally, we examine the stability of the equilibrium points for the circular restricted four-body problem with radiation pressure and found at least one positive real value or one positive real part of the eigenvalues (Table 1). Hence all the equilibrium points are unstable.

Acknowledgements

We are thankful to the Deanship of scientific research and the department of Mathematics, College of Science, Al-Zulfi, Majmaah University, Kingdom of Saudi Arabia for providing all the facilities in the completion of this research work.

References

[1]. Abdullah, (2017). Dynamics in the circular restricted three body problem with perturbations. International Journal of Advanced Astronomy. vol. 5, no. 1, pp. 19-25.

[2]. Abouelmagd, E. I., Sharaf, M.A., (2013). The motion around the libration points in the restricted three-body problem with the effect of radiation and oblateness. Astrophys. Space sci. vol. 344, pp. 321-332.

[3]. Abouelmagd, E. I., Mostafa, A., (2015). Out of plane equilibrium points locations and the forbidden movement regions in the restricted three-body problem with variable mass. *Astrophysics Space Sci.* 357, 58.DOI 10.1007/s10509-015-2294-7.

[4]. AbdulRaheem, A., Singh, J., (2006). Combined effects of perturbations, radiation and oblateness on the stability of equilibrium points in the restricted three-body problem. The Astronomical Journal. 131, 1880-1885.

[5]. Assis, S. C., et al., (2014). Escape dynamics and fractal basin boundaries in the planar earth-moon system, Celest. Mech. Dyn. Astr., 120, 105-130.

[6]. Baltagiannis, A.N., Papadakis, K.E. (2011). Equilibrium points and their stability in the restricted four-body problem. Int. J. Bifurc. Chaos 21, 2179.

[7]. Bhatnagar, K. B., Chawla, J. M., (1979). A study of the Lagrangian points in the photogravitational restricted three body problem. Indian journal of pure and applied mathematics. Vol. 10, pp. 1443-1451.

[8]. Chernikov, Yu. A., (1970). The Photogravitational restricted three body problem, Soviet Astronomy, 14(1), pp. 176-181.

[9]. Douskos, C. N., (2010). Collinear equilibrium points of Hill's problem with radiation pressure and oblateness and their fractal basins of attraction. Astrophys. Space Sci. 326, 263-271.

[10]. Kalvouridis, T., Arribus, M., Elipe, A., (2007). Parametric evolution of periodic orbits in the restricted four body problem with radiation pressure. Planetary and space science. Vol. 55, pp. 475-493.

[11]. Kumari, R., Kushvah, B. S., (2014). Stability regions of equilibrium points in the restricted four body problem with oblateness effects. Astrophysics Space Sci., 349, 693-704.

[12]. Lichtenegger, H., (1984) The dynamics of bodies with variable masses. Celest. Mech. 34, 357-368.

[13]. Meshcherskii, I.V., (1949). Studies on the Mechanics of Bodies of Variable Mass. *GITTL, Moscow.*

[14]. Mignard, F., (1984) Stability of L_4 and L_5 against radiation pressure. Celest. Mech. 34, 275-287.

[15]. Mittal, A., et. al., (2016) Stability of libration points in the restricted four-body problem with variable mass. *Astrophysics and space sci.* 361, 329. DOI 10.1007/s10509-016-2901-2.

[16]. Mccuskey, S. W., (1963). Introduction to Celestial Mechanics. *Addison–Wesley, USA.*

[17]. Perezhogin, A. A., (1976). Stability of the sixth and seventh libration points in the photogravitational restricted circular three body problem. Soviet Astronomy letters. Vol 2, pp. 172.

[18]. Pushparaj, N., Sharma, R. K., (2017). Interior resonance periodic orbits in the photogravitational restricted three-body problem. Advances in astrophysics. Vol. 1(2), pp. 25-34.

[19]. Sharma, R. K., (1987). The linear stability of libration points of the photogravitational restricted three body problem when the smaller primary is an oblate spheroid. Astrophys. Space Sci. vol.135, pp. 271-281.

[20]. Simmons, J. F. L., McDonald, A. J. C., Brown, J. C., (1985). The restricted three body problem with radiation pressure. Celestial Mechanics. Vol. 35, pp. 145-187.

[21]. Singh, J. et al. (1984). Effect of perturbations on the location of equilibrium points in the restricted problem of three bodies with variable mass. *Celest. Mech.* 32 (4), 297-305.

[22]. Singh, J., Ishwar, B., (1985). Effect of perturbations on the

stability of triangular points in the restricted problem of three bodies with variable mass. *Celest. Mech.* 35, 201-207.

[23]. Singh, J., Leke, O., (2010). Stability of photogravitational restricted three body problem with variable mass. *Astrophysics and Space Sci.* 326 (2), 305-314.

[24]. Singh, J., Leke, O., (2013). Existence and Stability of Equilibrium Points in the Robe's Restricted Three-Body Problem with Variable Masses. *International Journal of Astronomy and Astrophysics*. 3, 113-122.

http://dx.doi.org/10.4236/ijaa.2013.32013. .[25]

[26]. Singh J., Vincent, A. E., (2016) Equilibrium points in the restricted four-body problem with radiation pressure. Few-Body Syst. 57, 83-91.

[27]. Zhang, M. J., Zhao, C. Y., Xiong, Y. Q., (2012). On the triangular libration points in photo-gravitational restricted three body problem with variable mass. *Astrophysics Space Sci.*, 337, 107-113. DOI 10.1007/s10509-011-0821-8.

[28]. Zotos, E. E., (2016). Fractal basins of attraction in the planar circular restricted three body problem with oblateness and radiation pressure, Astrophys. Space Sci., 181, 17.

[29]. Zotos, E. E., (2016). Fractal basins boundaries and escape dynamics in a multi-well potential, Non-linear Dyn., 85, 1613-1633.

[30]. Zotos, E. E., (2016). Investigating the Newton-Raphson basins of attraction in the restricted three body problem with modified Newtonian gravity, J. Appl. Math. Comput., Oct., 1-19.

[31]. Zotos, E. E., (2017). Revealing the basins of convergence in the planar equilateral restricted four body problem, Astrophy. Space Sci., 362, 2